J Therm Anal Calorim (2009) 98:215–224
DOI 10.1007/s10973-009-0110-8

A thermogravimetic kinetic study of uncatalyzed diesel soot oxidation

Maria Kalogirou · Zissis Samaras

Received: 27 November 2008 / Accepted: 18 February 2009 / Published online: 28 August 2009

Abstract Isothermal and non-isothermal thermogravimetric experiments (TG) with real and synthetic (Printex U) soot were performed at different O_2 concentrations (5–22%O_2/N_2), sample masses (0.5–10 mg), heating (5–20 °C min^{-1}) and flow rates (80–100 mL min^{-1}). The significance of the experimental and calculation uncertainties (i.e. experimental parameter dependencies, calculation method and mass transfer limitations), which are related to TG for the extraction of chemical kinetics, was explored. Finally, an intrinsic kinetic equation for soot oxidation is proposed.

Keywords Kinetics · Oxidation · Soot · TG

Introduction

The use of diesel vehicles is increasing mainly due to their inherent advantages, which include fuel economy, durability etc. The main concern regarding their use are the increased nitrogen oxides and particulate matter (PM) emissions. Specifically, PM represents an important health hazard a fact that has led legislation to promulgation of stringent emission standards [1]. Diesel particulate filters (DPF) are becoming wide spread as an effective measure to reduce PM emissions as they have filtration efficiencies up to 100%. Due to the fuel penalty induced by the gradual loading of the filter, its periodical regeneration, i.e. the combustion of the accumulated particulates, is necessary [2]. Clearly, the achievement and control of this process are among the main challenges in DPF applications both for lifetime durability and fuel economy purposes. Consequently, the study of soot combustion for the extraction of chemical kinetics data that can be coupled in modelling tools is very important.

It is known that without any catalytic support soot is oxidized at substantial rates at temperatures higher than 550 °C under oxygen (O_2) [3]. In the literature there are numerous relevant studies and recommended oxidation mechanisms [e.g. 4–6]. The primary scope of these studies is the determination of soot mass reduction curve with respect to time or temperature. An Arrhenius type equation is then usually applied and activation energy, pre-exponential factor and reaction order with respect to oxidant and soot mass are thus evaluated. The basic challenges in this field are related with the sample and experimental setup characteristics. The commonly used synthetic soot samples are not necessarily equivalent to real diesel soot. Then again the quality of real soot is not constant and depends on engine and operational parameters. And, finally, the setup characteristics may impose uncertainties, such as rate controlling mass transfer limitations etc.

The experimental possibilities in this direction include full scale and mini-scale experiments and thermogravimetric analysis (TG). From full scale experiments to TG the procedure is simplified and more easily controlled but the conditions deviate from real world applications. Nevertheless, TG is considered an important tool and has been used extensively for soot oxidation studies [e.g. 4, 6]. It is a fast, economical and easy to use process, with the important advantage of the direct measurement of sample mass. On the other hand, TG has known experimental and computational difficulties which have led to extended criticism concerning the reliability of its results [7]. The extracted kinetics seem to depend on the experimental conditions [8], namely initial

M. Kalogirou · Z. Samaras (✉)
Laboratory of Applied Thermodynamics, Mechanical Engineering Department, Aristotle University Thessaloniki, P.O. Box 458, 541 24 Thessaloniki, Greece
e-mail: zisis@auth.gr

sample mass, heating rate etc., and the applied calculation method [e.g. 9]. And finally, mass transfer limitations may exist as the reaction gas is supplied to the solid sample through diffusion [e.g. 4]. These potential limitations evoke questions regarding the reaction regime, i.e. if the kinetics are in fact intrinsic. Keeping in mind that the kinetics used for modelling must only describe the reaction step, it is vital that they are free from such uncertainties.

In this context, goal of the present study is to explore the significance of the abovementioned uncertainties and to derive an intrinsic soot oxidation kinetic equation from TG experiments. The possibility to use the extracted data successfully in DPF modelling tools will be the object of an upcoming publication. In this direction, measurements were conducted using real and synthetic (Printex U) soot samples. Isothermal and non-isothermal tests were done at different O_2 concentrations (5–22% O_2/N_2), sample masses (0.5–10 mg), heating (5–20 °C min^{-1}) and flow rates (80–100 mL min^{-1}). The temperature range of interest was 550–700 °C. The reaction stoichiometry was determined through CO/CO_2 measurements at the TGA outlet. In order to explore the appearance of calculation artefacts, kinetic data from single non-isothermal curves were compared inter se and with the isothermal results. Additionally, the isoconversial Friedman method [10] was used for comparative purposes. Finally, reaction gas diffusion was explored and the mechanism that controls the reaction was determined. Photographic evidence is also provided for confirmation of the reaction regime.

Methodology

The experimental setup is presented in Fig. 1. A Perkin Elmer TGA 6 was used. The evolved gases were analyzed by a Horiba PG250 analyzer. Details about the setup are given in [11].

Both real diesel soot from a loaded DPF and synthetic soot (Printex U) were used. The protocols are described in Table 1. Lower masses were inevitably used for real soot experiments since its bulk density (~33 kg m^{-3}) was approximately half of that of Printex U (~66 kg m^{-3}). For the isothermal experiments the sample was heated to the reaction temperature under N_2 in order to avoid partial reaction and to allow the volatile fraction to desorb. Because of the slow gas change in the particular TGA a correction function developed in our laboratory was used in the calculations [11]. Non-isothermal experiments were conducted in the range 50–950 °C under the reaction gas. The volatile desorption in this case takes place during the experiment but at temperatures out of the range of kinetic interest, i.e. below 550 °C. CO/CO_2 was measured non-isothermally (20 °C min^{-1}) at 4.5, 14.9 and 22%O_2/N_2 for 5 mg Printex U and 3 mg Soot samples. Additional isothermal tests were conducted at 600, 625, 650 °C/22%O_2/N_2 only for Printex U.

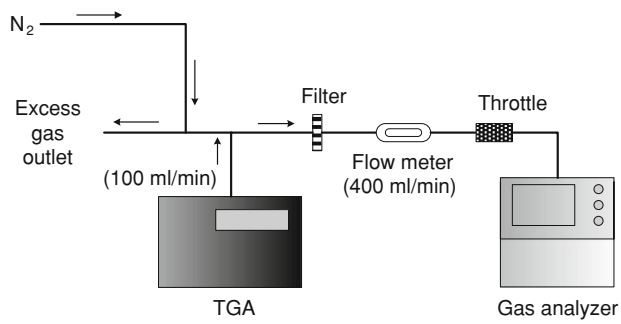

Fig. 1 Experimental setup

Kinetic formulations

The global reaction assumed to take place during soot oxidation under O_2 is:

$$C + \alpha_1 O_2 \rightarrow 2(\alpha_1 - 0.5)CO_2 + 2(1 - \alpha_1)CO \quad (1)$$

α_1 can take values between 0.5 and 1. α_1 can be determined from the ratio of CO and CO_2 concentrations (CO/CO_2 ratio) measured in the evolved gases. The conversion fraction (α) is defined:

$$\alpha = 1 - \frac{m}{m_o} \quad (2)$$

where m and m_o are the running and the initial sample mass, respectively. A 1st order with respect to mass kinetic model is assumed throughout this paper. This assumption is often made in literature [e.g. 6, 12] and is supported by experimental evidence presented in this paper. The reaction rate constant (k) is then defined:

$$k = \frac{1}{m} \cdot \frac{dm}{dt} = A \cdot \exp\left(-\frac{E}{RT}\right) \cdot [O_2]^n \quad (3)$$

A, E and n are the pre-exponential factor, activation energy and reaction order with respect to O_2, respectively. $[O_2]$ is the molar fraction of O_2 in the reaction gas. R, T and t are the universal gas constant, temperature and time, respectively. With n known, E and A can be determined by typical Arrhenius plots obeying the equation:

$$\ln\left(\left(\frac{1}{m} \cdot \frac{dm}{dt}\right) \Big/ [O_2]^n\right) = \ln\left(\frac{k}{[O_2]^n}\right) = \ln A - \frac{E}{RT} \quad (4)$$

n can be determined from the logarithmic form of Eq. 3 as follows:

$$\ln k = \ln A - \frac{E}{RT} + n \cdot \ln [O_2] = B + n \cdot \ln [O_2] \quad (5)$$

Since B is constant at a given temperature, n equals the slope of the ln k vs. ln O_2 linear plots. Thus, a value of n

Table 1 Protocols

Protocol	Sample	Flow-rate/mL min^{-1}	Sample mass/mg	Reaction gas/%	Heating rate (β)/°C min^{-1} or target temperature/°C
Isothermal	Printex U	105	0.5,1.5,5	4.5, 10.1, 14.9, 22	550, 575, 600, 625, 650, 700 °C
	Soot	105	0.5, 2		
Non-isothermal	Printex U	80,105	5, 10		5, 10, 20 °C min^{-1}
	Soot	80,105	2 (~3 in CO/CO_2 experiments)		

can be calculated for each investigated temperature. The arithmetic mean of these n values equals the global reaction order with respect to O_2 of the investigated reaction. This value in then used in Eq. 4 for the determination of the other kinetic parameters of interest (E, A). Alternatively n may be calculated from Arrhenius equations derived from non-isothermal experiments with different O_2 concentrations. Equation 5 may be rewritten as follows:

$$\ln k = \ln A + n \cdot \ln [O_2] - \frac{E}{RT} = C - \frac{E}{RT} \quad (6)$$

E/R and ln A are characteristic of the reaction and therefore constant. Consequently, the intercept C is a linear function of ln $[O_2]$. Thus, n equals the slope of the C vs. ln O_2 plots.

The least squares method was applied for all the necessary linear regression analyses for the purpose of the present paper.

Results and discussion

Kinetic equations

Isothermal measurements

Figure 2 presents typical k–α curves at 600 °C/22%O_2/N_2 for the two materials. Similar k were found for both samples. Also, k can be considered constant for the greater part of the reaction supporting the 1st order with respect to mass kinetic model assumption. Similar tendencies were observed for all test protocols. E calculation at different α levels revealed no E dependency on α, as can be seen for example in Fig. 3. Thus, k at $\alpha = 0.5$ were used as characteristic. The corresponding Arrhenius plots are presented in Fig. 4. Different markers were used in order to explore potential k dependency on initial sample mass. k seems to deviate slightly from linearity at temperatures above 650 °C, decreasing with increased mass. This could indicate the appearance of diffusional limitations in the porous sample which are discussed later. The phenomenon is more distinct for Printex U because of the larger mass variation. The derived kinetic equations from all test points are given in Table 2.

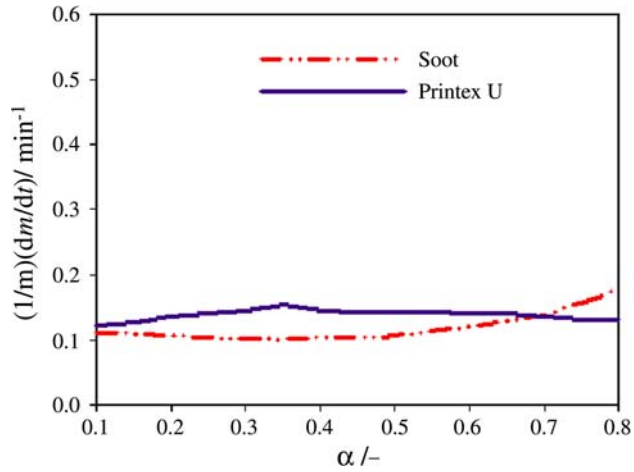

Fig. 2 Isothermally determined k at 600 °C/22%O_2/N_2 for soot and Printex U

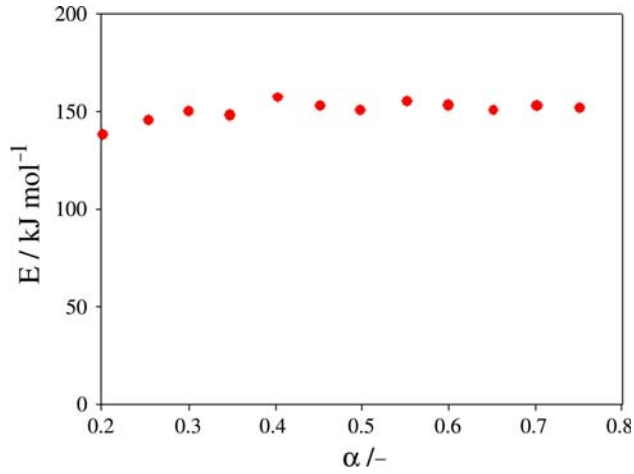

Fig. 3 Activation energy (E) data calculated from k values at different α levels for a Printex U (1.5 mg) oxidation experiment with 14.9%O_2/N_2

Non-isothermal measurements

The investigated temperature range is 550–700 °C. The non-isothermally measured k at 550–575–600–625–650 and 700 °C are presented together with the corresponding isothermal data in Fig. 5. Very good agreement is observed

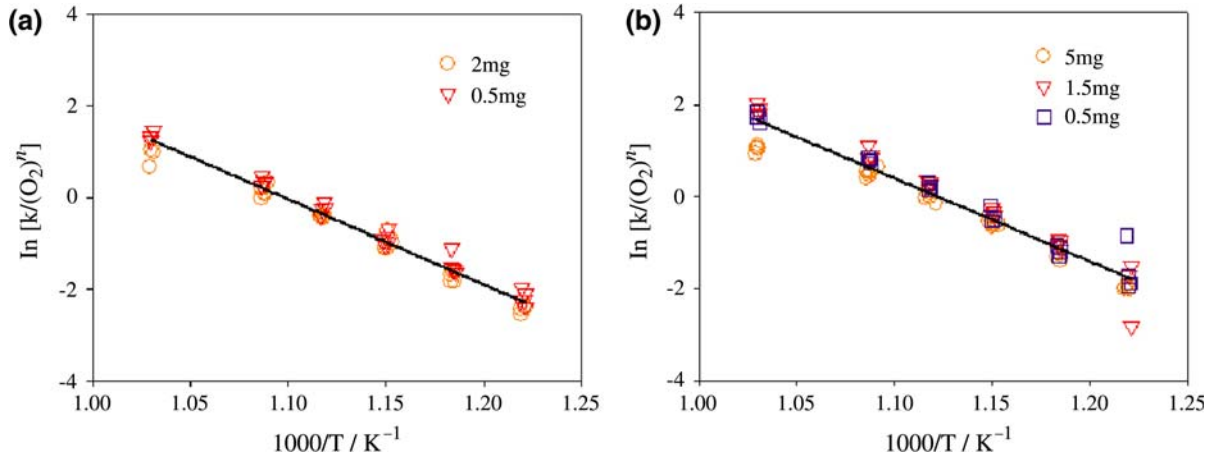

Fig. 4 Arrhenius plots (values at $\alpha = 0.5$ for all isothermal experiments). **a** Soot, **b** Printex U

Table 2 Summary of kinetic expressions

	Soot	Printex U
Isothermal k	$6.9 \cdot 10^8 \cdot \exp\left(-\frac{154229}{8.314 \cdot T}\right) \cdot [O_2]^{0.75}$, $R^2 = 0.98$	$5.9 \cdot 10^8 \cdot \exp\left(-\frac{149782}{8.314 \cdot T}\right) \cdot [O_2]^{1}$, $R^2 = 0.94$
Non-isothermal k	$1 \cdot 10^9 \cdot \exp\left(-\frac{158817}{8.314 \cdot T}\right) \cdot [O_2]^{0.75}$, $R^2 = 0.84$	$6.6 \cdot 10^8 \cdot \exp\left(-\frac{151315}{8.314 \cdot T}\right) \cdot [O_2]^{1}$, $R^2 = 0.91$
All test points	$1.72 \cdot 10^9 \cdot \exp\left(-\frac{161219}{8.314 \cdot T}\right) \cdot [O_2]^{0.75}$, $R^2 = 0.91$	$6.72 \cdot 10^8 \cdot \exp\left(-\frac{151492}{8.314 \cdot T}\right) \cdot [O_2]^{1}$, $R^2 = 0.91$

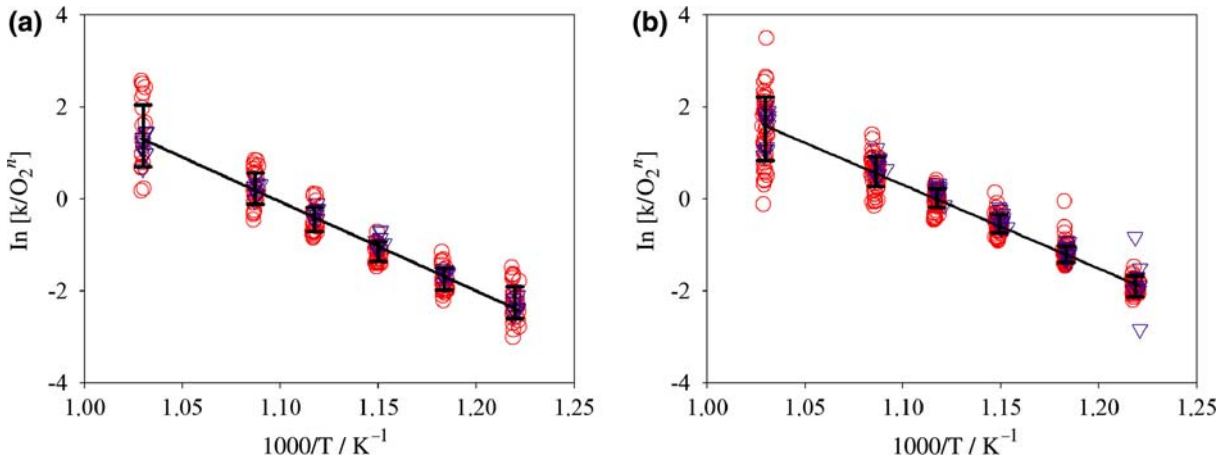

Fig. 5 Aggregated Arrhenius plots. The error bars correspond to one standard deviation of the values of all experimental points at every temperature (*inverted triangle* isothermal, *open circle* non-isothermal data): **a** soot, **b** Printex U

both for soot and Printex U. The kinetic equations derived from the non-isothermal data only and from all the test points can be found in Table 2. E was between 154–161 kJ mol^{-1} for soot and 149–151 kJ mol^{-1} for Printex U. This agreement reveals that the temperature protocol does not affect k results in the investigated temperature range.

It is then explored, if reliable kinetic data can be found from single non-isothermal curves, as often done in TG studies. First, the appearance of experimental parameter dependencies is explored. Figure 6 presents the α-temperature curves measured for three heating rates (β) and two initial masses at the highest and lowest concentration. Similar tendencies are observed for both samples. The curves are shifted to higher temperatures (higher than 700 °C in some cases) for increasing β irrespective of the other conditions. This trend is generally observed in TG curves and is usually attributed to thermal lag effects, e.g. [13]. Increasing the initial mass seems to affect the curves

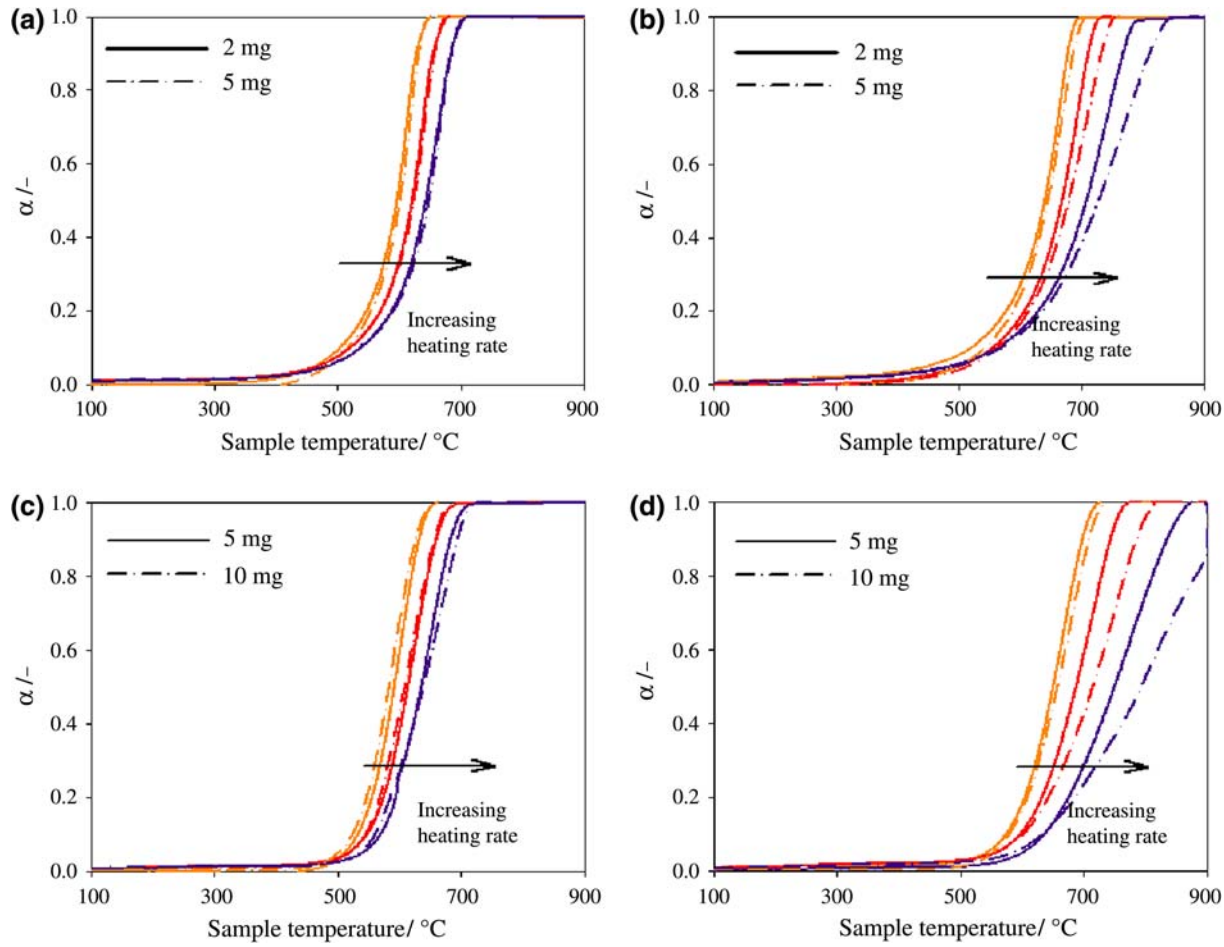

Fig. 6 α-temperature evolution for three β (5, 10 and 20 °C min^{-1}) and two sample masses: **a** soot, 22%O_2/N_2; **b** soot, 4.5%O_2/N_2; **c** Printex U, 22%O_2/N_2; **d** Printex U, 4.5%O_2/N_2

only in combination with lower O_2 concentrations in the reaction gas (e.g. in Fig. 6d) and especially for higher β, indicating the appearance of diffusional limitations. These trends were verified for all concentrations. E depended strongly on α and thus on the temperature range used in the calculations. For example, for soot oxidation at 10 °C/min/22%O_2/N_2, E was ~180 kJ mol^{-1} for α: 0.1–0.9 (corresponding to 520–660 °C) and 270 kJ mol^{-1} for α: 0.25–0.9 (585–660 °C), as can be seen in Fig. 7. All calculated E for α: 0.1–0.9 are presented in Fig. 8. The experimental conditions influence on the measured curves was also reflected on E in a similar manner. Hence, it is observed that β and sample mass affect the results in combination with lower concentrations. Moreover, the absolute E values presented significant scatter: they were between 140–200 kJ mol^{-1} for soot and 70–180 kJ mol^{-1} for Printex U. So, obviously, the calculated E are subjected to experimental and computational influences and no straightforward answer about the kinetics can be thus provided.

Next the results of the Friedman method [10] are discussed. As it is an iso-conversial method, its results were

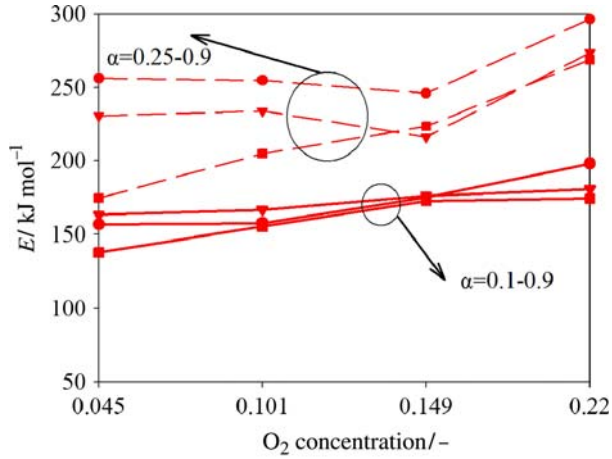

Fig. 7 E calculated from individual non-isothermal soot oxidation experiments for two α-ranges: 0.1–0.9 and 0.25–0.9 with respect to O_2 concentration (*filled circle* 5 °C min^{-1}, *inverted filled triangle* 10 °C min^{-1}, *filled square* 20 °C min^{-1})

based on the above discussed single curve data and were hence obviously influenced from the associated discrepancies. Thus, a great E scatter (50–200 kJ mol^{-1}) was

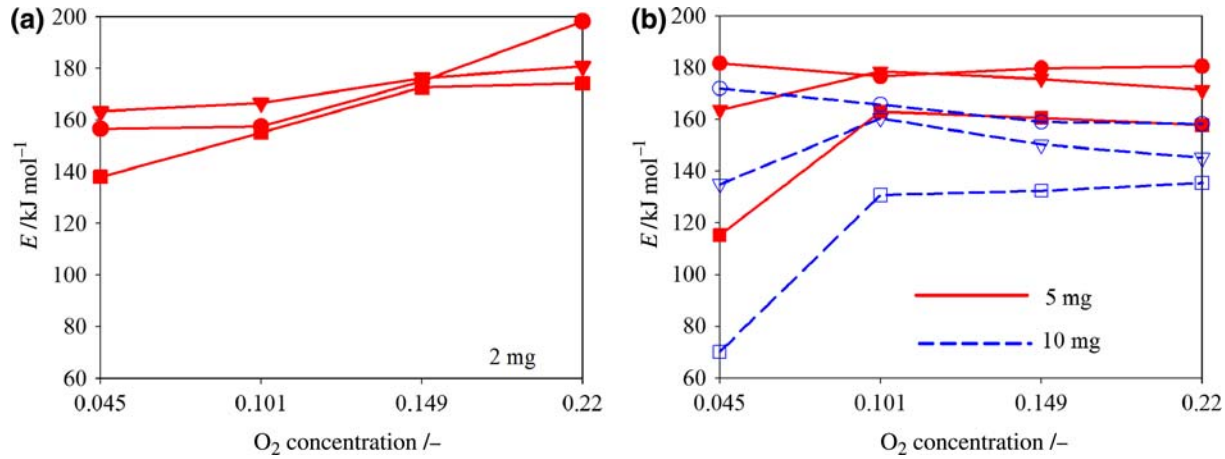

Fig. 8 *E* from individual non-isothermal experiments with respect to O_2 concentration (*filled circle* 5 °C min^{-1}, *inverted filled triangle* 10 °C min^{-1}, *filled square* 20 °C min^{-1}): **a** soot, **b** Printex U

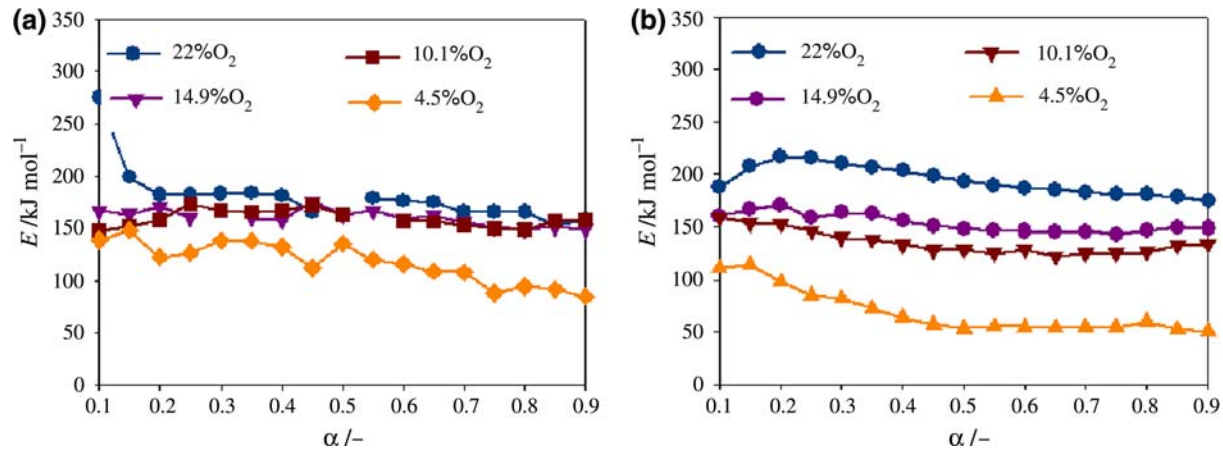

Fig. 9 *E* calculated from the Friedman method with respect to α **a** soot, **b** Printex U

observed for Printex U (Fig. 9b). More consistent but still ambiguous results were found for soot (Fig. 9a). A single *E* (~160 kJ mol^{-1}) could be determined between 10% and 22% O_2/N_2. Yet, it is not considered possible to provide a reliable global kinetic equation from this method.

Suggested kinetic equation

Taking into account: (a) the observed limitations of single curve analysis and Friedman method and (b) the consistency of the isothermally and non-isothermally determined *k* in the investigated temperature range, the kinetic equation extracted from all the test points is considered as characteristic for both samples (Table 2).

CO/CO_2 ratio

Isothermally measured CO/CO_2 for Printex U was independent of α. Very good consistency between the isothermally and non-isothermally measured ratios was observed (Fig. 10). It is, therefore, concluded that non-isothermal experiments can give reliable CO/CO_2 values. The corresponding results are presented in Fig. 11. For soot, CO/CO_2 was approximately 0.75 for all tested temperatures and concentrations. For Printex U, it did not depend on concentration but revealed an almost linear temperature dependency and was always greater than 1.

Diffusional limitations

The so far presented results indicate that chemical kinetics control the reaction (Regime I as defined for example in [14]). Specifically, *E* is in the range reported in literature for this regime, e.g. [15]. Furthermore, *k* is practically independent of α (Fig. 2), meaning that d*m*/d*t* is proportional to the running sample mass. This implies that the reaction takes place in the whole sample which is also characteristic of Regime I. This linear dependency is also

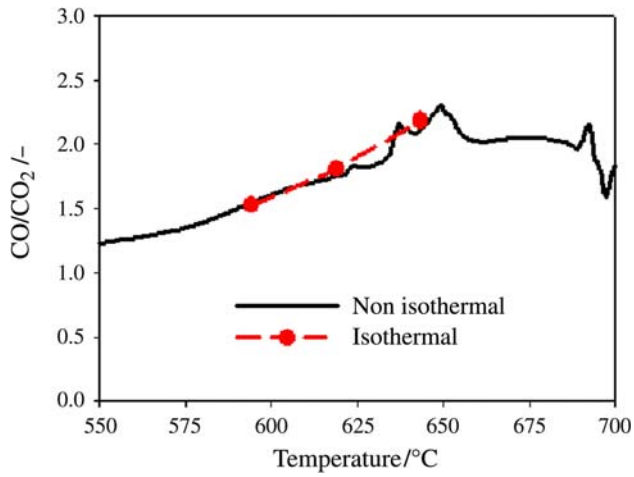

Fig. 10 Comparison of isothermally and non-isothermally measured CO/CO_2 ratios for Printex U

verified from the typical d*m*/d*t* vs. *m* plots presented in Fig. 12 and is valid for all test protocols. However, stress is given on the results at 650 °C/4.5%O_2/N_2 because these conditions of higher reaction rate and lower concentration are likely to impose diffusional limitations. To theoretically support these observations, the effectiveness factors (η) and the intrinsic reaction rate constants with respect to O_2 consumption (K) were determined using the methodology presented by Satterfield [16].

The effectiveness factor (η) represents the ratio of the global (measured) reaction rate over the intrinsic reaction rate, i.e. if the O_2 concentration in the whole porous sample equals the O_2 concentration on the sample surface. Should no diffusional limitations exist, then η tends to 1. For example, for a flat plate geometry and a first order irreversible reaction, η is given by an equation of the form [16, 17]:

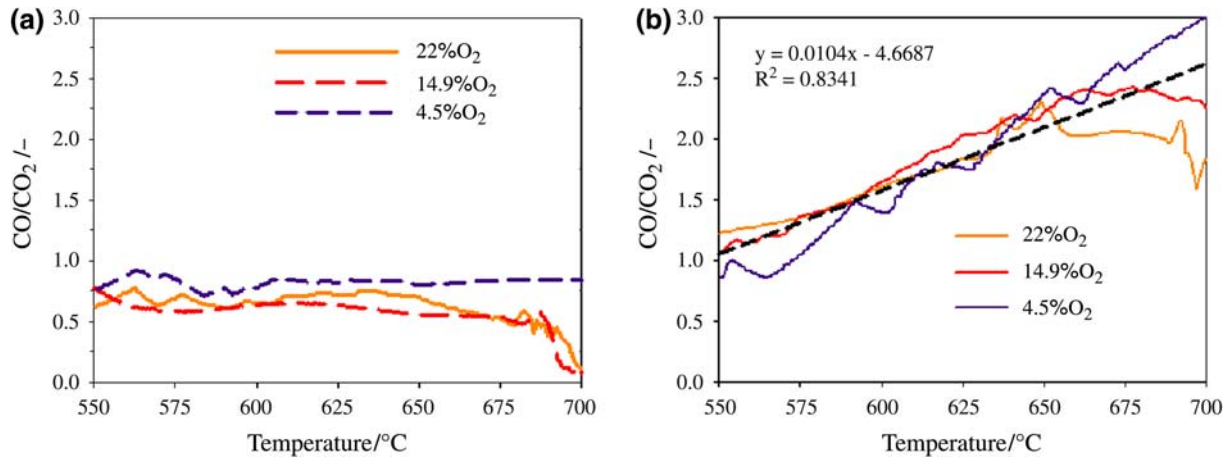

Fig. 11 CO/CO_2 with respect to temperature and O_2 concentration **a** soot, **b** Printex U

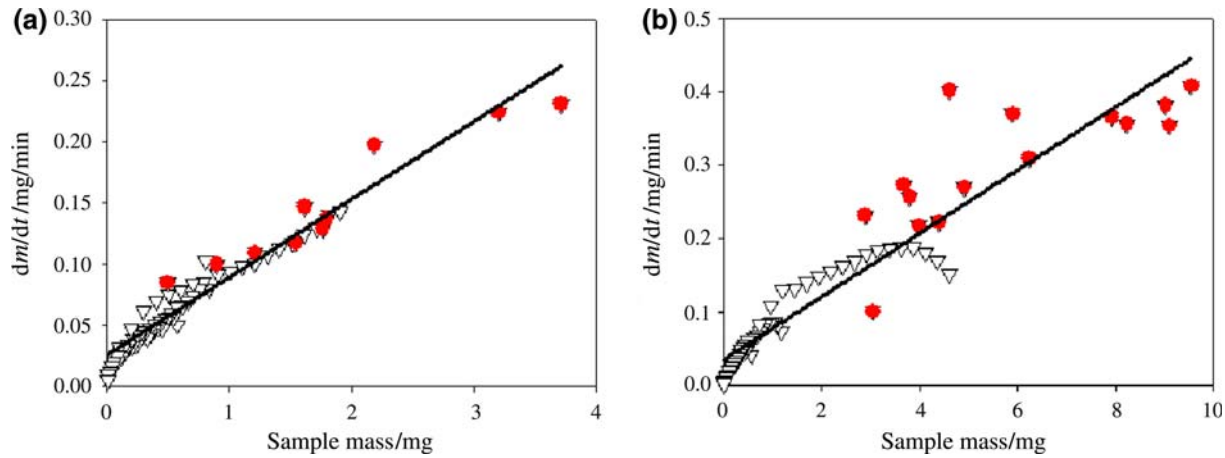

Fig. 12 Reaction rate (d*m*/d*t*) with respect to sample mass at 650 °C/4.5%O_2/N_2 (*filled circle* non-isothermal, *inverted triangle* isothermal) **a** soot, **b** Printex U

$$\eta = \frac{\tanh(\phi_L)}{\phi_L} \tag{7}$$

where ϕ_L is the Thiele modulus. This modulus is a measure of the significance of the diffusional limitations in the porous sample and can be expressed as follows [16]:

$$\varphi_L = L \cdot \sqrt{\frac{K}{D_e}} \tag{8}$$

where L is the pellet height, K is the intrinsic reaction rate with respect to O_2 consumption and D_e is the diffusion coefficient in the porous sample. When ϕ_L is relatively small chemical kinetics control the reaction. In order to determine ϕ_L and thus η, K must be known. In some cases, such as the present one, however, the appearance of diffusional limitations and the intrinsic K are not known a priori and have to be determined. In this direction, Satterfield [16] introduces a new magnitude, which combines the experimental data with ϕ_L and thus η:

$$\Phi_L = \frac{L^2}{D_e} \cdot R_v \cdot \frac{1}{y_s} = \left(\frac{L^2}{D_e} \cdot \mathrm{K} \cdot y_s^{m-1}\right) \cdot \eta = \varphi_L^2 \cdot \eta \tag{9}$$

where R_v [kg m^{-3} s^{-1}] is the global experimentally determined reaction rate. Thus it is possible to determine η and L from the experimental data.

In this direction the system geometry was simplified first for modelling (Fig. 13). A cylindrical pellet geometry was assumed. Its diameter was set equal to the crucible's, so that the same external surface (A_e) would be available for the reaction gas diffusion in both cases. Its volume was assumed equal to the crucible's, so that the pellet bulk density (ρ_b) and porosity (ε) would remain unchanged. Assuming constant ρ_b, the height (L) of the above described pellet of mass m_o can be calculated. Increasing the flow-rate did not influence the experimental curves in any case. Furthermore, smaller masses gave higher k (e.g. in Fig. 4b for $1000/T \sim 1.03$), although their surface is situated deeper in the crucible. Thus, it is expected that no external diffusional limitations exist and the O_2 concentration on the sample surface can be safely assumed equal to the bulk concentration. Fick's law and an empirical diffusivity (D_e) were used for the description of diffusion in the porous sample. The ratio of the mean pore diameter, as defined in [18], over the mean free path for O_2 was 6.5 for Printex U and 11 for soot. Therefore, Fickian diffusion could be considered the main diffusion mechanism for soot while that assumption had to be explored further for Printex U. D_e was 4.3–5.5 10^{-5} m^2 s^{-1} for soot and 4.2–5.4 10^{-5} m^2 s^{-1} for Printex U. Additional literature D_e values determined at the same porosity levels [18] were also tested for Printex U. They were extrapolated to the reaction temperatures using a $T^{1/2}$ dependency and were $\sim$1–1.09 10^{-5} m^2 s^{-1}. Next, the pellet size (L) and the corresponding dm/dt values had to be specified. For constant dm/dt (e.g. [4]), a single value can be assigned to the whole experiment and the initial mass can be used to calculate L. This was not the case in our study and pairs of dm/dt and m had to be defined, e.g. from Fig. 12. The intrinsic n were assumed equal to the experimental values, i.e. 0.75 for soot and 1 for Printex U. The reaction stoichiometry was calculated from CO/CO_2.

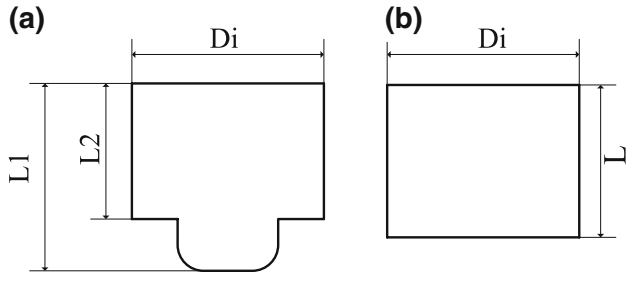

Fig. 13 Real (**a**) and equivalent (**b**) pellet geometry

In order for the calculated K to be intrinsic they must converge to a single value at every temperature, independently of sample size or O_2 concentration. This was also the criterion for the validation of the model assumptions. The calculated K at 650 °C are presented together with the experimental values in Fig. 14. Similar results were found for the other tested temperatures. For soot, K converge for $n = 0.75$. The corresponding η were always greater than 0.8 (including at 700 °C) and in the majority greater than 0.9. These values and the unvarying slope of the Arrhenius plot (Fig. 4a) support the conclusion that oxidation takes place in Regime I at the tested conditions. For Printex U only higher D_e (based on Fickian diffusion) led to convergence of K (Fig. 14b). In this case K practically did not depend on O_2 concentration meaning that 1 is the intrinsic n for Printex U. η were generally greater than 0.8 and between 0.9 and 1 for masses lower than 5 mg. For larger masses (>5 mg), η were lower, but in any case greater than 0.5, indicating conditions between regime I and II (i.e. when both chemical kinetics and pore diffusion control the reaction, as defined for example in [14]).

Finally, in order to experimentally verify the modelling results, sequential top and side view photographs were taken during oxidation of 5 mg Printex U samples at 650 °C/4.5%O_2/N_2. The crucible was removed from the balance for the side view photos and the furnace cover was opened for the top view ones. It should be emphasized that this process did not influence the measured k. The photos were taken at $\alpha \sim 0$, 0.4 and 0.8 and are presented in Fig. 15. It is observed that L remains unchanged and oxidation takes place internally, as in Regime I. So, the model calibration and the determined η are experimentally validated and the proposed kinetic data (Table 2) can be considered intrinsic.

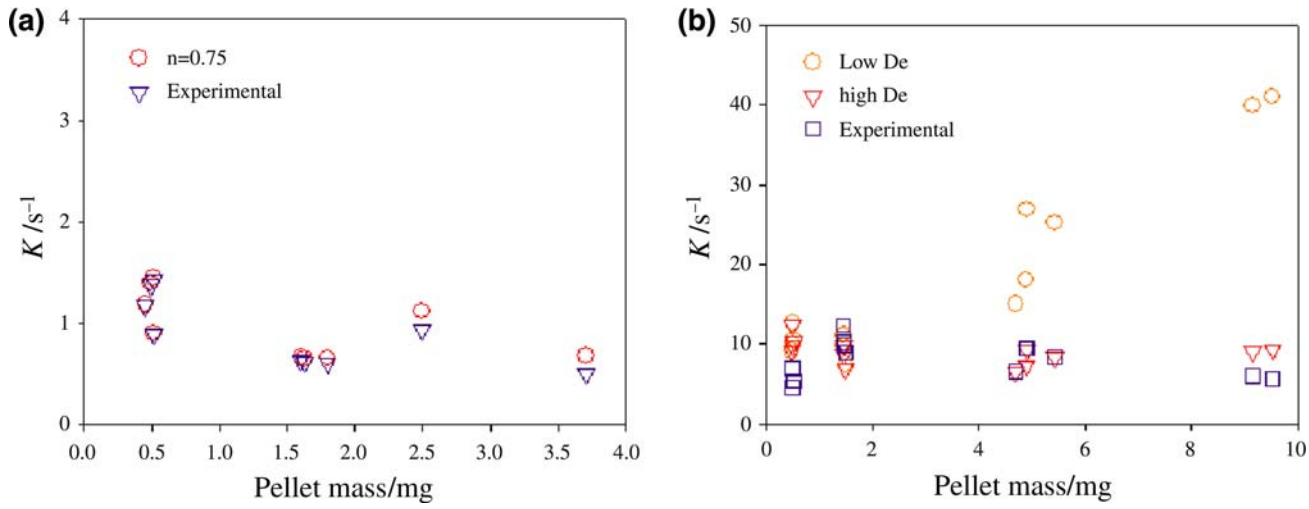

Fig. 14 Experimental and calculated K values at 650 °C **a** soot, **b** Printex U

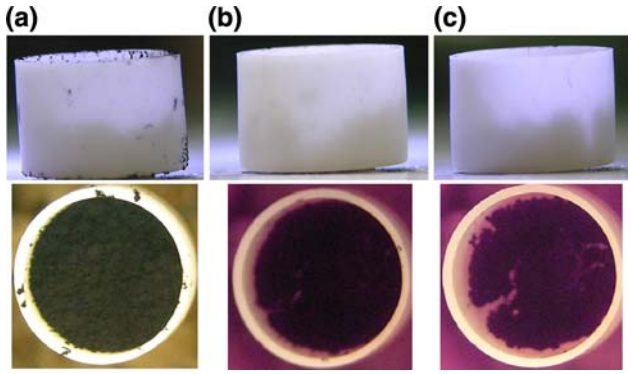

Fig. 15 Printex U (5 mg) oxidation (650 °C/4.5%O_2/N_2) photographs, at α: **a** 0%, **b** 40%, **c** 80%

Conclusions

Isothermally and non-isothermally determined k were consistent and resulted in comparable kinetic data between 550 and 700 °C. A 1st order with respect to sample mass kinetic model described soot oxidation accurately. No external mass transfer limitations were observed under the investigated conditions. η indicated that oxidation takes place in the kinetically controlled regime. Photographic experiments verified that the pellet height remains unchanged during oxidation, validating Regime I conditions. No straightforward kinetic data could be derived from the analysis of single non-isothermal curves or the Friedman method. The temperature range where oxidation took place and the form of the curves were subjected to experimental influences which distorted the calculated data in both cases. Smoother curves and better consistency were found for lower sample masses (<5 mg) and β (5 and 10 °C min^{-1}) especially for lower O_2 concentration and are recommended as appropriate test conditions. However, the application of single or multi-curve calculation methods should be done consciously and the kinetic equations should be extracted from k data in the temperature range of interest. The recommended expressions are:

$$\frac{1}{m}\cdot\frac{dm}{dt}[\mathrm{min}^{-1}] = 1.72\cdot 10^{9}\cdot\exp\left(-\frac{161219\,\mathrm{kJ/kmol}}{R\cdot T}\right)\cdot[O_2]^{0.75}$$

for soot

$$\frac{1}{m}\cdot\frac{dm}{dt}[\mathrm{min}^{-1}] = 6.72\cdot 10^{8}\cdot\exp\left(-\frac{151492\,\mathrm{kJ/kmol}}{8.314\cdot T}\right)\cdot[O_2]^{1}$$

for printex U

Finally, similar k were observed for both samples confirming previous findings [e.g. 15], that Printex U can be considered a valid soot surrogate. Yet, CO/CO_2 displayed different behaviour for the two materials. It was greater than 1 and depended strongly on temperature for Printex U while it was constant ($\sim$0.75) for soot. It did not depend on the O_2 concentration in any case.

Acknowledgements We would like to acknowledge the valuable contribution of P. Pistikopoulos and A. Tzilvelis, members of the laboratory staff, involved in the experimental study. We also acknowledge the financial support of the Greek State Scholarship Foundation (IKY).

References

1. Dieselnet. What are diesel emissions. www.dieselnet.com/tech/emi_intro.html.
2. Dieselnet. Diesel filter regeneration. www.dieselnet.com/tech/dpf_regen.html.
3. Stanmore BR, Brilhac JF, Gilot P. The oxidation of soot: a review of experiments, mechanisms and models. Carbon. 2001; 39:2247–68.

4. Gilot P, Bonnefoy F, Marcuccilli F, Prado G. Determination of kinetic data for soot oxidation. Modeling of competition between oxygen diffusion and reaction during thermogravimetric analysis. Combust Flame. 1993;95:87–100.
5. Illeková E, Csomorová K. Kinetics of oxidation in various forms of carbon. J Therm Anal Cal. 2005;80:103–8.
6. Stratakis GA, Stamatelos AM. Thermogravimetric analysis of soot emitted by a modern diesel engine run on catalyst-doped fuel. Combust Flame. 2003;132:157–69.
7. Galwey AK. Eradicating erroneous Arrhenius arithmetic. Thermochim Acta. 2003;399:1–29.
8. Roduit B, Maciejewski M, Baiker A. Influence of experimental conditions on the kinetic parameters of gas-solid reactions—parametric sensitivity of thermal analysis. Thermochim Acta. 1996;282–283:101–19.
9. Brown ME, Maciejewski M, Vyazovkin S, Nomen R, Sempere J, et al. Computational aspects of kinetic analysis: part A: the ICTAC kinetics project-data, methods and results. Thermochim Acta. 2000;355:125–43.
10. Friedman HL. Kinetics of thermal degradation of char-forming plastics form thermogravimetry. Application to phenolic plastic. J Appl Poly Sci C. 1965;6:183–95.
11. Kalogirou M, Pistikopoulos P, Ntziachristos L, Samaras Z. Isothermal soot oxidation experiments with intermediate gas change in a Perkin-Elmer TGA6. J Therm Anal Cal. 2009;95:141–7.
12. Yezerets A, Currier NW, Eadler HA. Experimental determination of the kinetics of diesel soot oxidation by OD2—modelling consequences. SAE technical paper, 2003, 2003-01-0833.
13. Liu C, Yu J, Sun X, Zhang J, He J. Thermal degradation studies of cyclic olefin copolymers. Polym Degrad Stab. 2003;81:197–205.
14. Walker PLJ, Rusinko FJ, Austin LG. Gas reactions of carbon. Adv Catal. 1959;11:133–221.
15. Neeft JPA, Nijhuis TX, Smakman E, Makkee M, Moulijn JA. Kinetics of the oxidation of diesel soot. Fuel. 1997;76:1129–36.
16. Satterfield CN. Mass transfer in heterogeneous catalysis. Cambridge, MA: MIT Press; 1970.
17. Smith JM. Chemical engineering kinetics. New York: McGraw-Hill Inc; 1981.
18. Brilhac JF, Bensouda F, Gilot P, Brillard A, Stanmore B. Experimental and theoretical study of oxygen diffusion within packed beds of carbon black. Carbon. 2000;38:1011–19.